Research Square

Preprints are preliminary reports that have not undergone peer review.
They should not be considered conclusive, used to inform clinical practice,
or referenced by the media as validated information.

Reciprocating-Rotating mixer-based Powder Delivery System Giving Continuous Metal Particles Flow in Aqueous Media during Powder-based Electrochemical Metal Additive Manufacturing

Wondwosen Demisse
Hayden Brown
Amy M. Elliot
Pawan Tyagi
ptyagi@udc.edu

University of the District of Columbia https://orcid.org/0000-0002-7541-1344

Research Article

Keywords: Additive manufacturing, 3D printing, Mechanism, Metal, Flow Simulation, Powder Transportation

Posted Date: May 9th, 2026

DOI: https://doi.org/10.21203/rs.3.rs-9546340/v1

License: This work is licensed under a Creative Commons Attribution 4.0 International License.
Read Full License

Version of Record: A version of this preprint was published at The International Journal of Advanced Manufacturing Technology on October 5th, 2026. See the published version at https://doi.org/10.1007/s00170-026-19248-2.

Reciprocating-Rotating mixer-based Powder Delivery System Giving Continuous Metal Particles Flow in Aqueous Media during Powder-based Electrochemical Metal Additive Manufacturing

Wondwosen Demisse[1] · Hayden Brown[1], Amy Elliott [2] · Pawan Tyagi[1*]

Corresponding Author (*): ptyagi@udc.edu

[1.] Mechanical Engineering, University of the District of Columbia, 4200 Connecticut Avenue NW, Washington, DC 20008, USA
[2.] Oak Ridge National Laboratory, Manufacturing Demonstration Facility, 2350 Cherthala Boulevard, Knoxville, TN 37932, USA

Abstract: This study introduces an innovative metal powder transportation mechanism designed specifically for deployment within a Powder-based Electrochemical Metal Additive Manufacturing (PECAM). The PECAM invention is a desktop metal additive manufacturing machine that produces a wide range of composites at near-room temperatures, under ambient conditions, and with a fraction of the energy required compared to laser metal sintering-based additive manufacturing. A major roadblock to realizing PECAM was particle clogging at the nozzle exit. We invented a novel engineering mechanism for continuously dispensing metal powder at a controllable rate into aqueous media from the nozzle of the PECAM system, without clogging (Pending U.S. Patent Application for Apparatus and Method for Wet Powder Dispensing for Low Temperature Metal 3D Printing, Patent Application #20240399463). PECAM, with a novel powder-dispensing method, represents a critical advancement in the field of metal additive manufacturing, offering a cheaper (like a plastic 3D printer) system that operates near room temperature and yields unprecedented composites in which particles and coating metals can be chosen arbitrarily. This paper discusses the use of a reciprocating-rotating system to transport metal powder for PECAM processes. The proposed system introduces a mixing motion that facilitates the seamless transportation of particles through channels inside a liquid medium while minimizing issues such as particle choking and clogging. A particle transport simulation using Altair EDEM is conducted to assess the forces involved and calculate the system's flow rate. The findings from this study contribute to enhancing the efficiency and reliability of metal powder transportation for the wide range of applications of PECAM. This study will also provide an initial platform for developing the Digital Twin framework to further advance and apply PECAM-impacting metal additive manufacturing.

Keywords Additive manufacturing; 3D printing; Mechanism; Metal; Flow Simulation; Powder Transportation

1. Introduction:

Powder feed mechanisms play a crucial role in powder processing industries like chemical, food, pharmaceuticals, and additive manufacturing (AM) [1-3]. The need to dispense powders or mixtures of powders occurs in a wide range of industries. The list of applications includes the preparation of pharmaceutical products, the mixing of pigments for paints, inks, and glazes, the incorporation of processing additives and pigments into polymer processing lines, and in solid free forming processes[4, 5]. A model was developed for predicting the feed factor profile of a powder, processed through a gravimetric feeder, as a function of material properties and process parameters[6]. Their primary function is to transfer powders from a storage container or hopper to downstream processing units like mixers, reactors, or spray guns. Yang et. al. [4] have presented an exhaustive review of different powder dispensing technologies and mechanisms. Powder sintering, Laser, and E-Beam energy have been used to melt and fuse the powder particles to additively manufacture formerly unthinkable complex designs into functional components. On the other hand, binder jetting is a metal additive manufacturing method that first adds the metal powder with the help of resin into a component's desired shape. In the next step, the resin is replaced with a low-melting alloy (Yc) that is pushed or sucked between the particles in the liquid

form to yield a coating around the metal particles(Xp). Upon solidification, the overall volume of the green-binder-jetted component shrinks by a few tens of percent, yielding the desired shape of the XpYc composite. The binder jetted additive manufacturing (BJAM) approach is economical and requires 400-600 °C temperature range; however, many variables need to be controlled to produce the final product. Laser sintering and binder jetting-based AM processes both require extensive equipment, rigorous process control, and skilled technicians and researchers to operate successfully. A new revolution will occur if metal additive manufacturing can be performed at near-room temperature using a desktop metal 3D printer. Electrochemical deposition-based additive manufacturing has been proposed and attempted. However, the deposition rate is limited by the maximum achievable electroplated film thickness given the maximum current available in the electroplating solution. Limitations of electrochemical plating-based metal 3D printing can be resolved if the microscopic dimensions of the metal powder are the rate-determining step. Here, we demonstrate a novel additive manufacturing technology developed by local in situ binding of the dispensed metal particle to yield novel composite materials and metals. We recently disclosed a PECAM concept that relies on uninterrupted dispensing of metal particles from a nozzle at the desired location. Several methods were employed to prototype PECAM. Commonly employed methods of transportation systems include screw feeders, disk feeders, pneumatic systems, vibration systems, and gravity-driven mechanisms. These transportation systems are widely used and are prevalent means of conveying materials or objects across industries [7, 8].

Screw feeders are one of the most commonly used types of powder feed mechanisms in powder processing industries [9]. They are favored because of their reliability, accuracy, and flexibility [10]. The working mechanism of a screw feeder can be divided into four stages, namely, filling, conveying, metering, and discharging [9, 11]. During the filling stage, the hopper gets filled with powder material, and the screw rotates to create a void in the hopper. The conveying stage involves the movement of powder along the screw length while compressing and densifying it towards the discharge port. In the metering stage, the screw rotates at a controlled speed to deliver a precise amount of powder to the downstream processing unit. In the discharge stage, the powder is discharged from the screw through a discharge port into the processing unit. While screw feeders are preferred for simplicity, they can be susceptible to clogging and require regular cleaning and maintenance to ensure optimal performance [12].

Disk feeders are a kind of powder feed system that utilizes a rotating disk for conveying powders from a hopper to a downstream processing unit [13]. The operating mechanism of the disk feeders consists of three main stages: filling, dosing, and discharge. During the filling stage, the hopper is loaded with powder, and the rotating disk creates a void in the hopper. First, the powder flows into the void, and the disk keeps rotating until the hopper is full. During the dosing stage, the disk rotates, propelling the powder along its surface toward the discharge port. Then the dosing volume is determined by the disk speed and the depth of the powder layer. In the discharge stage, the powder is released from the disk through a discharge port and into the processing unit. Disk feeders are extensively used in applications that require precise dosing and controlled powder flow, such as the pharmaceutical and food industries [14]. The main benefits of disk feeders comprise their ability to handle a broad range of powder types, ease of cleaning and maintenance, and low noise levels. Nevertheless, they can also be restricted by their lower dosing capacity and may need extra measures to avoid clogging [15].

Pneumatic systems use air pressure to move powders from a hopper to a processing unit. The process is divided into three stages: convey, separation, and discharge. The compressed air creates a high-velocity stream to transport the powder, with flow controlled to maintain a consistent flow rate [16]. The powder and air are separated using a cyclone or filter, and the powder is collected in a receiver for discharge into the processing unit. Pneumatic systems are useful for transporting powders over long distances and in hazardous environments. They have high transport efficiency, can handle various powder types, and require low maintenance. However, they have high energy consumption, may require additional measures to prevent powder degradation or loss, and are not suitable for wet environments [17].

Vibration systems transport powders from a hopper to a processing unit using mechanical vibrations. The process can be divided into two stages: convey and discharge. The vibrating platform moves the powder toward the discharge port during the conveying stage. The amplitude and frequency of vibrations can be adjusted to ensure a consistent flow rate. In the discharge stage, the powder is transported to the processing unit [18]. Vibration systems are ideal for handling fragile or abrasive powders in the food and pharmaceutical industries. They are easy to operate and maintain, consume less energy, and have lower transport capacity. Additional measures may be required to prevent powder segregation or bridging [19].

Gravity-driven systems are an economical and straightforward means of moving powders from a hopper to a processing unit [20]. The mechanism operates in two stages: filling and discharging. During the filling stage, the hopper is filled with powder, which is then transported via a gravity-fed chute to the discharge port. The powder flow rate is determined by the chute's size and angle. In the discharging stage, the powder is released from the chute and into the processing unit. These systems are useful for small-scale processing or laboratory settings where simple, low-cost powder transport is required. They are user-friendly, consume less energy, and are suitable for handling a wide range of powder types [21]. However, they have a lower transport capacity and may require additional measures to prevent powder

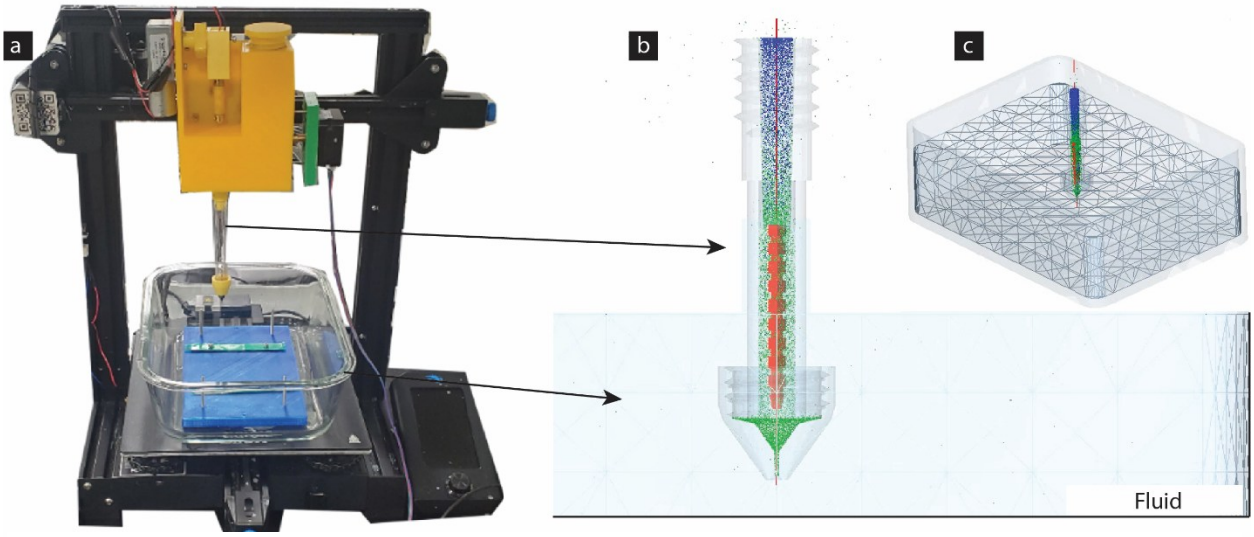


Fig. 1: (a) Prototype of powder based electrochemical additive manufacturing(PECAM) enabled by choking proof powder delivery mechanism in the liquid media by including a Nozzle with mixer(b) Mixer in the Nozzle simulated (c) within the bath.

segregation or bridging.

This paper will discuss the invention of a novel metal powder dispensing apparatus designed for the PECAM application (Fig. 1a). A powder dispensing system (Fig. 1b) in a wet environment enabled synchronized particle motion through a nozzle in the electrolyte solution for in situ bonding at the landing site. Here, we also present a deeper mechanistic understanding of the forces and key factors underlying the microscopic behavior of the powder dispensing system, specifically designed for metal 3D printing at near-room temperature in an open environment without requiring an inert gas or a vacuum. This paper focuses on industry-grade Finite Element simulation of powder flow through the actual CAD model used in prototyping (Fig. 1c). We also demonstrate successful powder-based metal 3D printing using our novel metal powder dispenser.

2. Design and Functioning of PECAM Powder Dispenser:

Figure 2 illustrates the complete powder delivery system that was embedded in our prototype (Fig. 1a) and simulated using Finite Element Analysis (Fig.1b-c). The integration of a powder dispenser into the

fully developed prototype is discussed elsewhere in this paper. Here, we discuss the powder flow from the container to the substrate, in which powder particles are bonded by additive manufacturing via electrochemical coating. Transparent front view of the PECAM powder delivery method involving three motors (Fig. 2a). Stage 1 of powder flow involves pushing the powder from the reservoir tank into a glass tube at a controllable rate with the help of a stepper motor. This operation is facilitated by the integration of gravity and a screw conveyor. The Nema17 stepper motor is coupled to a screw with a 10 mm pitch.

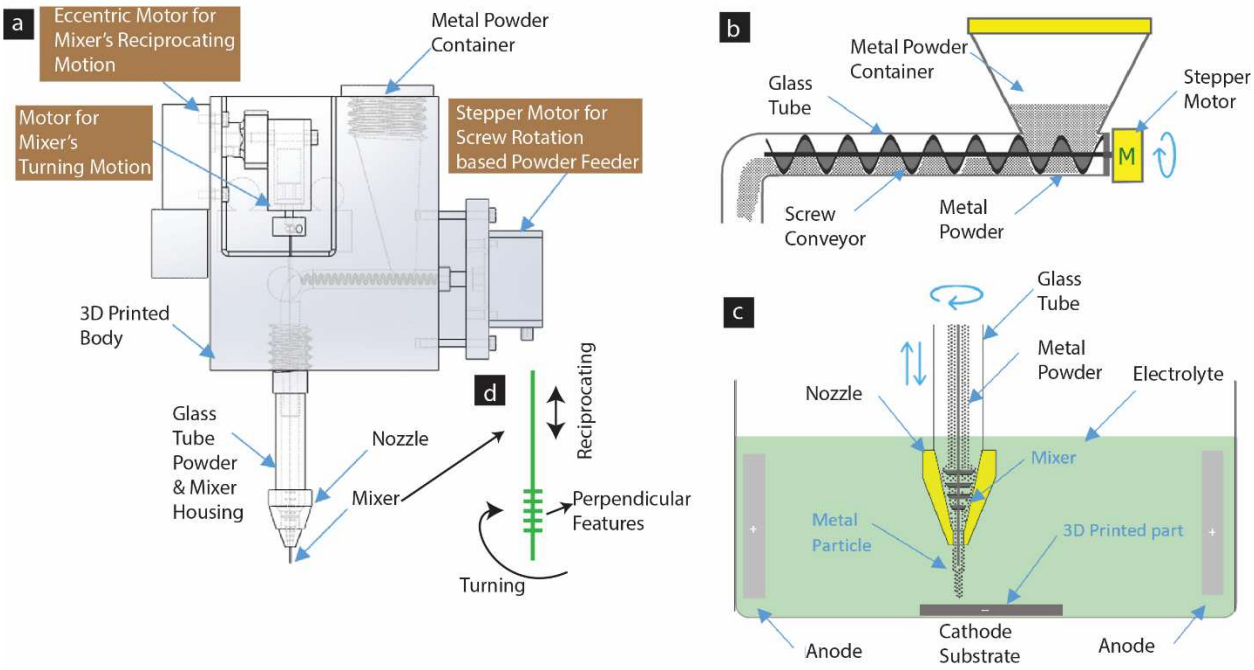


Fig 2. (a) Transparent front view of the PECAM powder delivery method involving three motors, (b) powder motion from reservoir to nozzle's glass tube via screw conveyor actuated by stepper motor, and (c) Reciprocating-Rotating mechanism for mixer rod to facilitate smooth powder delivery at desired site.

The continuous rotation of the motor generates a void, enabling the seamless transport of powder from the metal powder container (Fig. 2b). This flow control from the reservoir is achieved by manipulating various parameters. The first parameter involves adjusting the screw pitch diameter: increasing the pitch diameter increases the flow rate, and conversely, reducing it diminishes the flow rate. The second avenue for regulating flow involves manipulating screw speed, measured in revolutions per minute (RPM). As with pitch diameter adjustments, an increase in RPM increases flow rate, while a decrease reduces it. The third parameter pertains to introducing a delay that momentarily halts the motor, thereby interrupting the powder flow. Upon reaching the terminus of the screw, the powder is pushed into a vertical glass tube, thereby initiating the commencement of the second stage (Fig. 2a).

Powder particles subsequently fall into the tube under gravity and start traveling around the mixer rod (Fig. 2c). The Mixer rod is custom-designed by spot welding the perpendicular features on the lower part (Fig. 2d). The Mixer rod is continuously moving up and down in such a manner that perpendicular features always travel up to the narrow region of the nozzle without smashing. The section below the perpendicular feature is designed to be long enough to travel beyond the nozzle exit and enter the liquid bath to ensure that powder particles are cleared regularly from the nozzle inner volume (Fig.2c). Synchronized reciprocating-rotating motion of the mixer rod facilitates smooth powder delivery at desired site during PECAM based additive manufacturing on the substrate (Fig. 2c). The reciprocating and rotation motion of the mixer is shown in figure 2d without powder or housing for clear view.

Perpendicular features on the mixer (Fig. 2d) are included to break the powder lumps forming right above the small diameter nozzle exit (Fig.1b). While the extended length of the mixer can travel up and down through the nozzle to keep pushing the metal powder in the wet media (Fig. 2c). The rotational movement is designed to induce a vortex motion, ensuring an even and consistent amalgamation of the powder and electrolyte. Simultaneously, the reciprocating motion facilitates unobstructed flow of the mixture, mitigating the risk of clogging at the exit nozzle (Fig. 2c). The system perpetually mixes the powder and electrolyte, thereby optimizing the seamless transit of the mixture through the nozzle. Notably, the presence of an electrolyte containing the metal ion of the coating to be produced around each particle is the fundamental necessity of the PECAM mechanism. Hence, the mixer's role is critically important in ensuring the availability of electrolytes around each particle as it lands on the substrate, where additive manufacturing will occur. Without a mixer, a lump of powder that is wet on the outside and dries on the inside lands on the substrate, and no additive manufacturing occurs.

3. Simulation study

Understanding the science of powder flow via the novel Nozzle for PECAM is critically essential for mechanistic understanding. However, experimentally determining the forces acting on thousands of metal particles under the mixer's reciprocating and rotational motion is extremely challenging.

A suitable semi-empirical model is to define powder flow rate as the sum of a gravity-fed baseline plus mixer-enhanced transport from rotation speed and reciprocation speed:

$$Q_p = Q_0 + k_1\omega + k_2 fA + k_3 \omega fA$$

Where: Q_p= powder flow rate, for example particles/s or g/s
Q_0= baseline gravity-driven flow rate without mixer motion
ω= mixer rotational speed, rad/s or rpm
f= reciprocation frequency, Hz
A= reciprocation stroke amplitude, m or mm
fA= characteristic reciprocation speed
k_1, k_2, k_3= empirical constants obtained from experiment or EDEM simulation

The most important term is the interaction term $k_3\omega fA$ because clog prevention likely depends on the combined effect of rotation-induced mixing and reciprocation-induced nozzle clearing, not either motion alone. A more physically meaningful version could be:

$$Q_p = \rho_b A_n v_{eff}$$

with: $$v_{eff} = v_0 + \alpha\omega R + \beta fA + \gamma(\omega R)(fA)$$
Hence, $$Q_p = \rho_b A_n [v_0 + \alpha\omega R + \beta fA + \gamma(\omega R)(fA)]$$

Where: ρ_b= bulk powder density
A_n= nozzle exit area
R= mixer radius or effective swept radius
v_0= gravity-driven velocity contribution
α, β, γ= fitting coefficients

The powder flow rate may be modeled as a function of rotational speed and reciprocation speed using a coupled transport relationship in which the effective particle velocity is governed by gravity, rotation-induced mixing, reciprocation-induced clearance, and a nonlinear interaction between the two mixer motions.

To examine the interaction of metal particles within the system and their response to the environment, we conducted Finite Element simulations of our PECAM nozzle design using Altair® EDEM™ software [22]. EDEM is a high-performance Finite Element software for bulk and granular material simulation (Fig.1b-c). The Discrete Element Method (DEM) enables accurate simulation and analysis of particle behavior. This simulation method has been used to understand the flow of granular materials such as coal, mined ores, soils, fibers, grains, tablets, etc., through industrial equipment. The EDEM simulation provided crucial insight into how those materials will interact with the different sections of the equipment

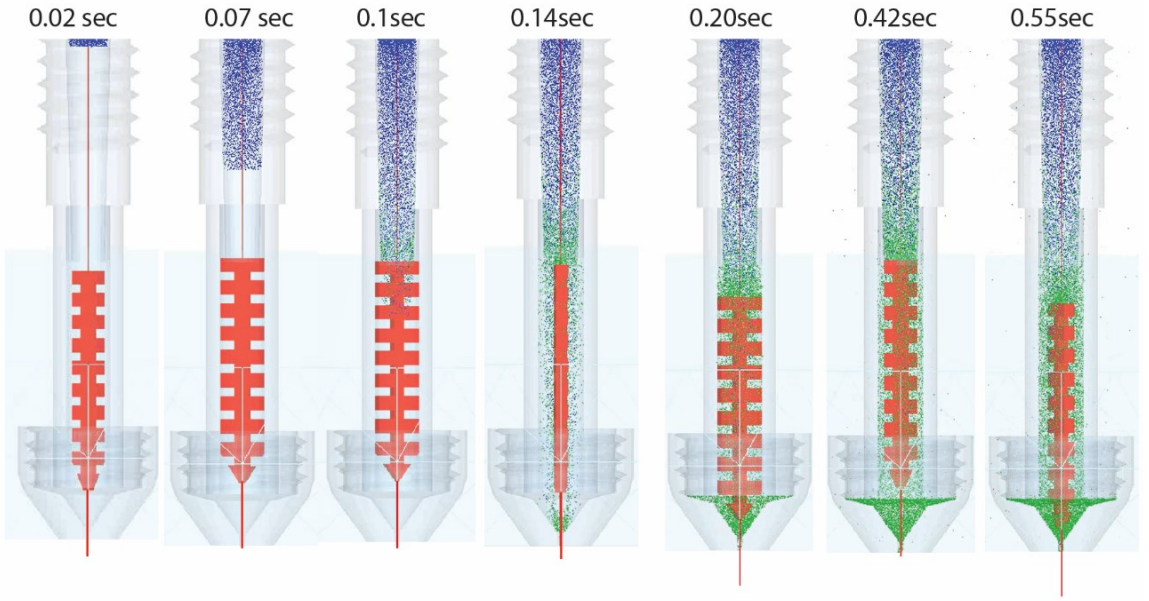


Figure 3: EDEM simulation showing particles flow at different time stage under the mixer influence.

across a range of operating and process conditions.

The simulation serves as a valuable tool for comprehending the forces generated within the glass tube, nozzle, and mixer to mobilize powder particles (Fig. 1b). For realistic simulation, we produced a CAD model of the exact nozzle and glass tube that is used in the functional PECAM prototype to simulate actual system (Fig. 3a). This dynamic interplay arises from the rotational and reciprocating motions of the mixer. The simulation conditions are as follows. The 3D-printed nozzle is represented as a plastic material in the simulation and has a 1mm diameter exit. In the EDEM simulation, we set a gravity-fed flow rate of 100,000 particles/sec and modeled the actual powder material and shape using 25 µm-

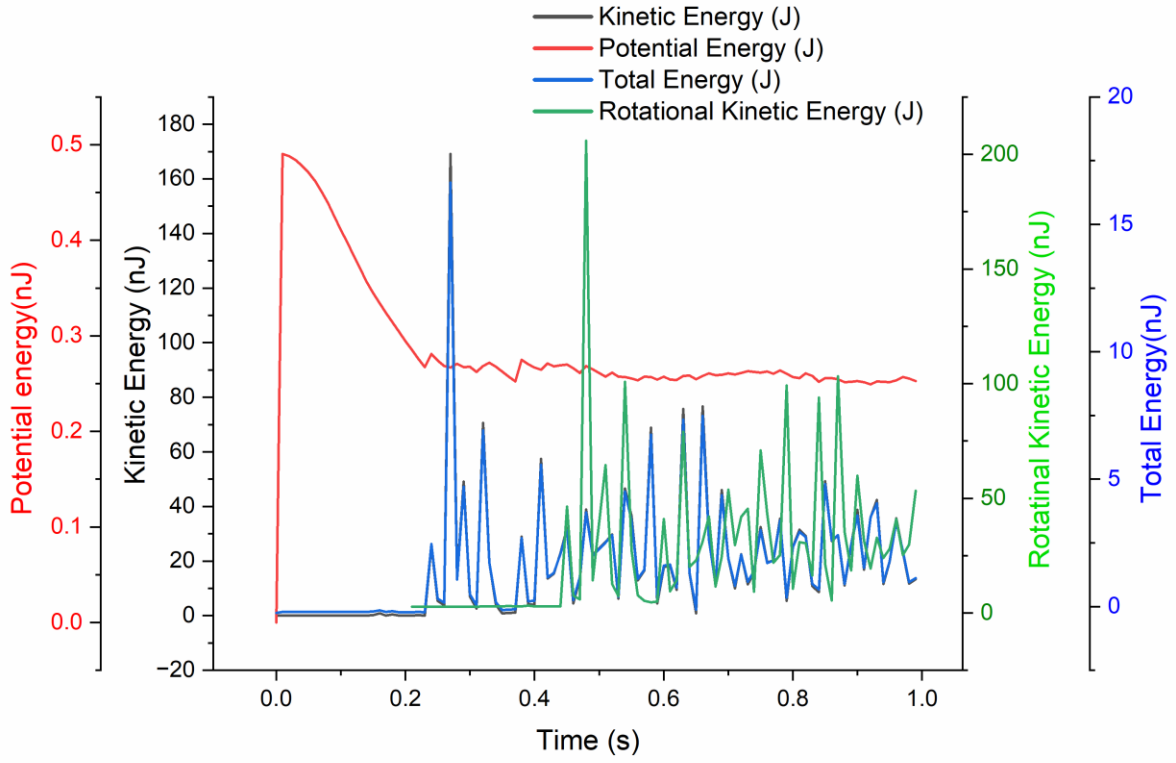


Figure 4: Potential, kinetic, rotational kinetic, and total energy of the particles at different time stages.

diameter spherical steel powder. The simulation is conducted at room temperature and in ambient settings. The simulation includes the motion of the mixer with the welded horizontal wire. The mixer moved up and down by 4 mm at 3 Hz and rotated at 350 rpm.

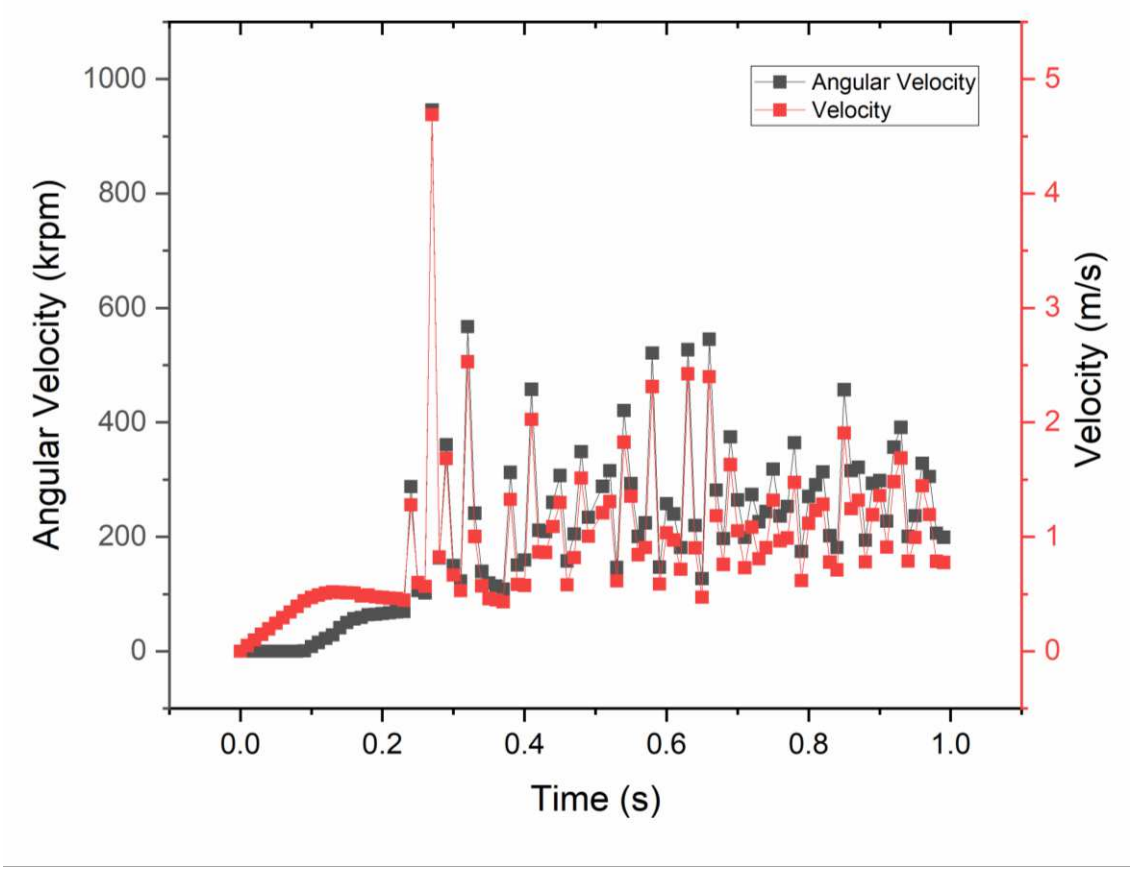


Figure 5: Angular and linear velocity of the particles at different time stages.

Figure 3 shows the flow of particles from the top of the glass tube under gravity and the impact on the mobile mixer. Blue color particles are unimpacted by the mixer. However, green particles are influenced by the mixer motion. We analyzed several parameters over a period of one second, during which 20,000 particles passed through the nozzle. We investigated the energy of the particles passing through the glass tube and then the nozzle as a function of time (Fig. 4). The potential energy of particles passing through the glass tube in the very beginning was the highest since many particles could travel the whole 100 mm distance due to a clear path (Fig. 3, around t=0.02 sec). However, as particles began to accumulate, they traveled shorter distances before hitting the floor created by the particles in the mixer region. Particles in the mixer region. Hence, particles dissipate, decreasing potential energy by up to 0.2 sec. It also means that particle buildup reaches a rather steady state around the mixer body within the first 0.2 sec (Fig. 3, images from 0.02 to 0.2 sec). After 0.2 seconds, the steady buildup of particles in the tube only allowed free-fall from the entrance to near the mixer's top (Fig. 3). It is noteworthy that kinetic energy and rotational kinetic energies are insignificant in the first 0.2 seconds (Fig.4). After that, the mixer's reciprocating and rotational motion provide force to move the entire particle population around the mixer. It is noteworthy that the magnitude of the particles' kinetic energy is ~10 times that of the potential energy. For this reason, total particle energy closely follows the trajectories of rotational kinetic and kinetic energy. It is apparent that the mixer's rotational and reciprocating motions translate into changes in kinetic and rotational kinetic energy (Fig. 4).

We also evaluated the linear and angular velocities of the particles at different time points (Fig. 5). The analysis of angular velocity over time reveals dynamic trends in the dataset. In the first 0.1 seconds, the angular velocity rapidly increases from 0 RPM to 7210.46 RPM, indicating significant acceleration. This

rapid increase continues into the subsequent 0.1 seconds, with the velocity reaching 67138.4 RPM by 0.2 seconds. Beyond this initial phase, from 0.3 to 0.8 seconds, the angular velocity continues to rise steadily but at a more moderate rate, reaching 418530 RPM by 0.8 seconds. Throughout this interval, there are noticeable fluctuations in velocity, with increases at specific time points such as 0.41 seconds (543139 RPM) and 0.56 seconds (496586 RPM), and decreases at 0.78 seconds (213522 RPM) and 0.79 seconds (187093 RPM). This analysis highlights the complex and evolving nature of angular velocity over time, characterized by initial rapid acceleration, followed by more gradual changes with intermittent fluctuations in velocity.

The comparison between the time-versus-angular-velocity (RPM) and time-versus-velocity (m/s) datasets reveal insights into the dynamics of rotational and linear motion. It is noteworthy that initial increases in linear velocity and near-zero angular velocity are attributed to the stage of particle build-up around the mixer. Both datasets demonstrate similar trends in acceleration and speed changes over time, despite representing different types of motion. The rapid increase in angular velocity (from 0 RPM to 7210.46 RPM within the first 0.1 seconds) corresponds to a comparable rise in linear velocity (from 0 m/s to 0.46975 m/s). This alignment underscores fundamental principles of motion dynamics, in which changes in speed—whether rotational or linear—are governed by a common physical origin arising from the mixer's synchronized rotational and reciprocating motion. By examining these datasets together, we gain a comprehensive understanding of how speed evolves over time in different motion contexts, providing valuable insights into the behavior of rotating and linearly moving systems.

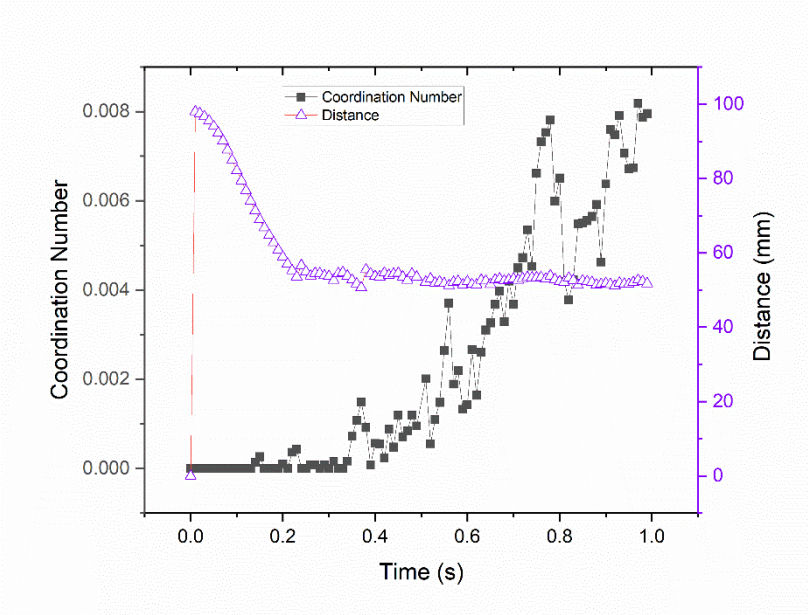


Figure 6: Coordination number and average distance traveled at different time stages.

The analysis of particle movement in a 100 mm-long tube with a narrow nozzle at the bottom reveals intriguing trends across different time intervals. Between 0.01 and 0.2 seconds, the distance traveled by particles steadily decreases from 97.98 mm to 58.74 mm, indicating a consistent reduction in particle movement during this period. The initial 97.98 mm distance traveled by the particle corresponds to the scenario shown in Figure 3 at t=0.02 seconds, where the initial group of particles travels the full tube length. In contrast, the trend between 0.2 and 0.99 seconds shows greater variability, with the particle distance initially stabilizing around 58.74 mm before fluctuating within a range. The maximum distance traveled within these time spans differs notably: 97.98 mm at 0.01 seconds, being the highest within 0.01 to 0.2 seconds, and 55.70 mm at 0.31 seconds, being the peak within 0.2 to 0.99 seconds. This analysis suggests that particle motion initially slows significantly but then becomes more complex, with fluctuations and varying maximum distances as time progresses beyond 0.2 seconds. Between 0.2 and 0.99 seconds, the distance traveled by particles appears to stabilize initially around 58.7436 mm (at 0.2 seconds). Then it fluctuates within a range, reaching a maximum of 55.70 mm at 0.31 seconds and a minimum of 50.53 mm at 0.6 seconds, before eventually increasing to a peak of 53.20 mm at 0.99 seconds. It is noteworthy that the difference

between 55.70 mm at 0.31 seconds and a minimum of 50.53 mm at 0.6 seconds is similar to the mixer vertical stroke length of 4 mm set in the EDEM simulation. Overall, the study provides insights into the dynamics of particle flow in confined spaces and highlights the evolution of particle trajectories over time.

In the context of particles falling in a 100 mm-long vertical tube with a 1 mm-diameter nozzle, the coordination number is the ratio of particles that successfully pass through the nozzle to the total number of particles. The coordination number data reflect how this ratio changes over time as the particles interact with the tube and nozzle system (Fig. 6). We compared the coordination number trends across the time intervals 0.01 to 0.2 seconds, 0.2 to 0.6 seconds, and 0.62 to 0.99 seconds.

1. **Between 0.01 and 0.2 seconds**: The coordination number during this interval remains relatively low, with values ranging mostly from 0 to approximately 0.001. There are sporadic small peaks and fluctuations in the coordination number, indicating the initial settling of particles and limited passage through the nozzle.

2. **Between 0.2 and 0.6 seconds**: In this time range, from 0.2 to 0.6 seconds, there is a noticeable increase in the coordination number. The values start to rise consistently and reach higher levels, ranging from approximately 0.001 to 0.007. This suggests that the particle flow and passage through the nozzle become more efficient over this interval due to the continuous action of the mixer in the lower half of the tube.

3. **Between 0.62 and 0.99 seconds:** Continuing from the previous interval, between 0.62 and 0.99

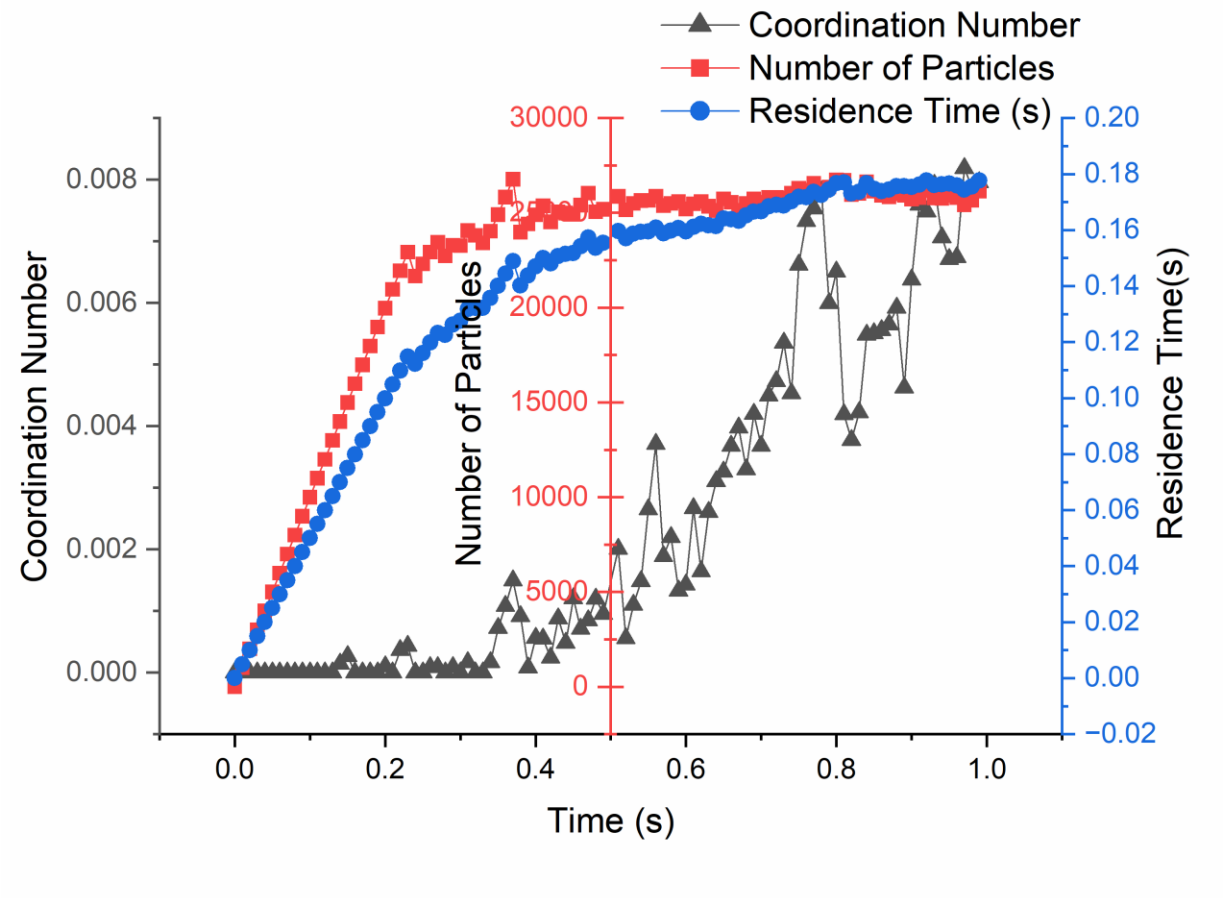


Figure 7: Coordination number, number of particles, and particles' residence time at different time stages.

seconds, the coordination number continues to increase and stabilize. The values remain relatively high, ranging from 0.002 to 0.008, indicating a sustained improvement in particle throughput and clearance through the nozzle. This steady increase in the coordination number reflects the mixer's ongoing effectiveness in facilitating particle flow and preventing blockages within the tube-and-nozzle system.

Overall, the comparison shows a progression from low coordination numbers during the initial phase (0.01 to 0.2 seconds) to higher and more stable coordination numbers as the system operates over longer time intervals (0.2 to 0.6 seconds and 0.62 to 0.99 seconds). This trend underscores the dynamic nature of particle movement and clearance within the tube, driven by the mechanical action of the mixer and the evolving flow dynamics of the particle system. This analysis suggests that the particle flow and passage through the nozzle become more efficient over time, likely due to the continuous operation of the mixer in the lower half of the tube, which helps clear the nozzle and break down any particle lumps that could impede flow. The increasing coordination number indicates improved particle throughput and clearance through the nozzle as the system stabilizes and particle dynamics adjust to the mixer's action.

Largely, the comparison highlights the critical role of the mixer in optimizing particle flow and clearance in the tube system. While gravitational effects and obstruction by the mixer body may impede particle movement (reducing the distance traveled over time), the mixer's coordinated action improves the overall efficiency of particle passage through the nozzle, as evidenced by increasing coordination numbers over time. This dynamic interplay underscores the importance of effective design and operational strategies for maintaining optimal performance in particle-handling systems within confined vertical spaces.

The analysis of time-versus-residence-time data for particles falling through a 100 mm vertical tube with a 1 mm nozzle and a rotating mixer reveals insightful trends across distinct time periods. Initially, from 0 to 0.2 seconds, the residence time steadily increases as particles encounter challenges passing through the nozzle, possibly due to interactions with the mixer or internal tube dynamics that affect their flow. This prolonged residence time indicates initial settling and passage difficulties experienced by the particles within the system. Subsequently, during the period from 0.2 to 0.6 seconds, the residence time stabilizes, showing minimal fluctuation around 0.1 seconds. This stability suggests a more consistent flow pattern as the particles overcome the initial settling phase, facilitated by the mixer's continuous action, which breaks down lumps and promotes smoother particle passage through the nozzle. However, as we progress from 0.62 to 0.99 seconds, a slight increasing trend in residence time is observed again. This trend implies that, despite ongoing mixer operation, variability in particle-flow dynamics or nozzle-clearance effectiveness may affect the residence time. The findings underscore the importance of continuous monitoring and adjustment of mixer parameters to maintain consistent particle flow and prevent operational issues over extended time periods in vertical tube configurations with narrow nozzles and internal mixers.

We have analyzed the time versus particle number data alongside the previously discussed time versus residence time and time versus coordination number data (Fig. 7). Looking at the time versus particle number data, we observe a steady increase in the number of particles over time, starting from 1000 particles at 0.01 seconds and increasing linearly up to 10000 particles at 0.1 seconds. Beyond 0.1 seconds, the rate of particle increase continues, with some variation, reaching around 26000 particles by 0.99 seconds. Comparing this with the time versus residence time data, we see a similar trend in the initial phase (0 to 0.2 seconds) where the residence time increases gradually from 0 seconds to approximately 0.1 seconds. This indicates that particles are spending more time within the tube during this phase, possibly due to increased density and slower flow. In the later phase (0.2 to 0.99 seconds), the residence time remains relatively stable, around 0.15 to 0.18 seconds. In contrast, the time-versus-coordination-number data show a different pattern. The coordination number, which represents the degree of aggregation or clustering of particles, starts from zero and gradually increases over time. In the initial phase (0 to 0.2 seconds), the coordination number remains very low, indicating minimal aggregation. However, between 0.2 and 0.99 seconds, the coordination number increases significantly, suggesting

greater particle aggregation or clustering, possibly due to interactions facilitated by the mixer in the lower half of the tube. Cumulatively, these comparisons highlight different aspects of particle behavior in the vertical tube with a nozzle and a mixer. The particle number steadily increases over time; the residence time varies but stabilizes after an initial phase; and the coordination number indicates changes in particle aggregation, particularly influenced by the mixer in the tube's lower half.

We also simulated and analyzed the torque experienced by particles. Analyzing the time-versus-torque data for the tube with a nozzle and rotating mixer provides insight into the mechanical forces and dynamics within the system. The torque values start from zero at the initial time (0 seconds) and remain negligible up to 0.09 seconds. After this point, there is a notable increase in torque values, albeit still relatively small (in the order of 10^{-19} to 10^{-16} N/m) up to around 0.3 seconds. From 0.3 seconds onwards, the torque values begin to fluctuate and increase significantly, reaching higher magnitudes (in the order of 10^{-11} to 10^{-12} N/m) up to 0.99 seconds. The torque values reflect the influence of the rotating mixer within the lower half of the tube. Initially, minimal torque is exerted, indicating a stable or inactive mixer state. However, as time progresses, particularly beyond 0.3 seconds, the torque values show greater variability and increase, suggesting increased mechanical agitation and particle mixing within the tube. This agitation contributes to the observed trends in particle behavior, residence time, and coordination number discussed earlier, influencing particle movement, aggregation, and flow dynamics within the tube system. The torque data underscores the importance of mixer dynamics in shaping the overall behavior and characteristics of particle movement and interaction within the vertical tube system.

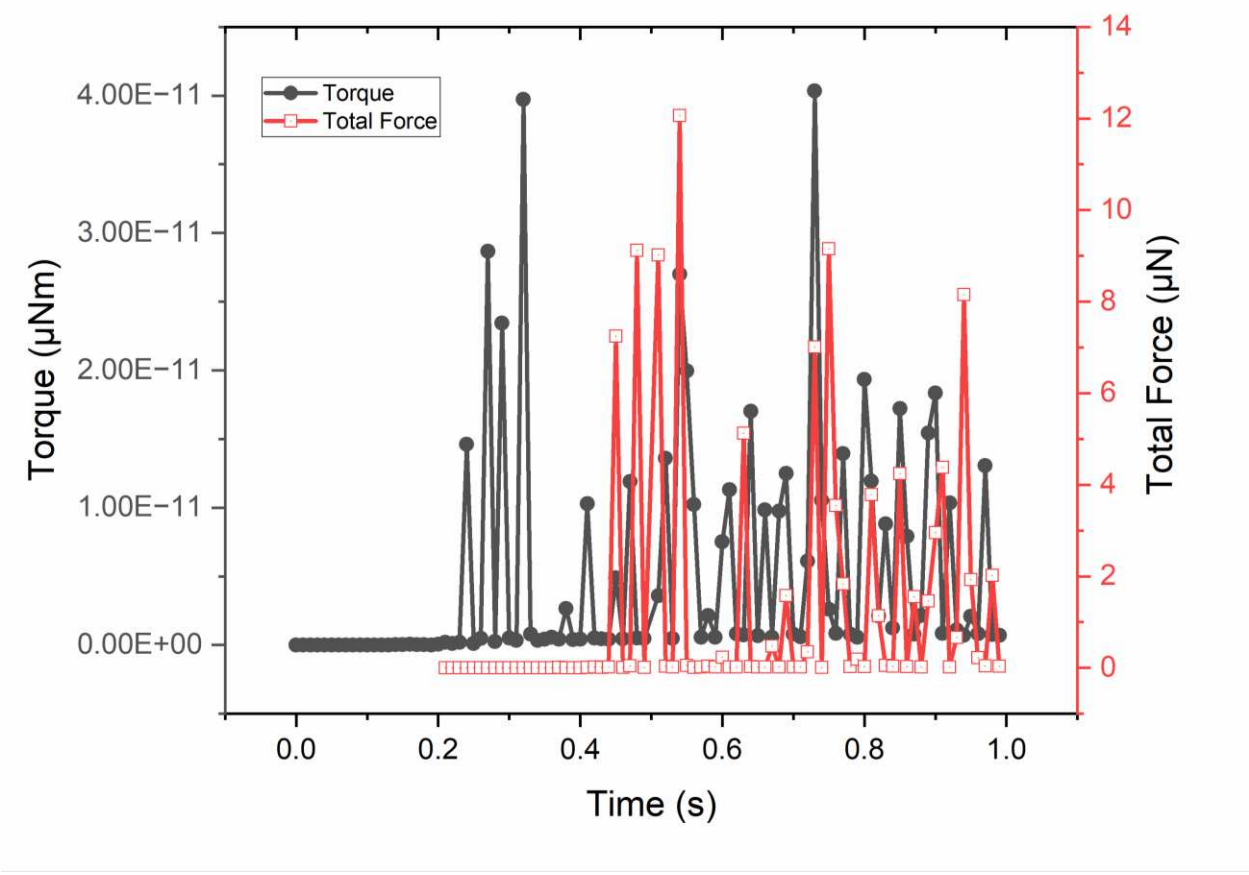


Figure 8: Torque and total force variation at different time stages.

In addition to torque, we analyzed the time-versus-total-force data for powder particles passing through a vertical tube with a nozzle and a rotating mixer (Fig. 8). Initially, at t=0 seconds, the total force is zero,

indicating the absence of external or applied forces. As time progresses, particularly after t=0.1 seconds, the total force values increase gradually, albeit at relatively low magnitudes (in the range of 10^{-9} to 10^{-8} N). From t=0.3 seconds onwards, there is a noticeable increase in total force values, with fluctuations and occasional spikes (up to 10^{-5} N) observed. These increases in force likely reflect the dynamic behavior of the rotating mixer, which exerts mechanical forces on the particles and influences their movement within the tube. The trends observed in the total force data align with the patterns seen in other related datasets, such as torque, particle number, residence time, and coordination number, highlighting the interconnected nature of mechanical dynamics and particle behavior within the tube system.

4. Conclusions

This study presents a comprehensive Discrete Element Method (DEM)-based investigation of powder transport dynamics within a novel, patent-pending reciprocating–rotating mixer system designed for Powder-Based Electrochemical Additive Manufacturing (PECAM). The primary objective was to establish a mechanistic understanding of particle behavior in a confined liquid-assisted nozzle environment, where conventional powder delivery systems typically fail due to clogging and unstable flow. The simulation results reveal that particle transport undergoes a clear transition from an initial gravity-dominated regime to a dynamically stabilized flow regime governed by the mixer's synchronized reciprocating and rotational motion. During the initial phase, particle motion is characterized by high potential energy and limited interaction with the mixer. As the system evolves, mixer-induced agitation significantly increases particle kinetic and rotational energies, thereby enhancing mobility and continuous particle circulation within the nozzle.

Key performance indicators, including coordination number, residence time, particle velocity, and force interactions, demonstrate that the mixer effectively mitigates particle agglomeration and promotes sustained throughput. The observed increase and stabilization of coordination number over time confirm improved particle passage through the nozzle, while relatively stable residence times indicate consistent flow behavior. Additionally, the evolution of torque and force distributions highlights the critical role of mixer kinematics in maintaining particle motion and preventing clog formation.

Importantly, the results validate the fundamental operating principles of the patent-pending wet powder dispensing mechanism (U.S. Patent Application #20240399463), demonstrating its ability to deliver continuous, controllable, and clog-resistant powder in aqueous media. The integration of reciprocating and rotational motion not only enhances flow reliability but also ensures adequate mixing between powder particles and electrolytes, which is essential for success in situ electrochemical bonding during PECAM processes.

Overall, this work provides a physics-based framework for understanding and optimizing powder delivery in liquid-phase additive manufacturing systems. The insights gained from this study establish a foundation for future development of digital twin models and enable systematic optimization of design and operating parameters. These advancements are expected to significantly enhance the scalability, reliability, and material versatility of PECAM, contributing to the broader adoption of low-temperature, energy-efficient metal additive manufacturing technologies.

Acknowledgments

Author contributions: PT conceived the PECAM concept, while Wondwosen explored various designs and refined the existing one. Additionally, Wondwosen conducted system simulations using Altair EDEM software, and Betelhiem performed data analysis and interpretation.

Funding: This research was funded by the National Science Foundation CREST Award, grant number HRD- 1914751, Department of Energy/ National Nuclear Security Agency (DE-FOA-0003945), and

NASA MUREP Institutional Research Opportunity Grant under Cooperative Agreement #80NSSC19M0196. Amy Elliot Funding

Availability of data and materials. The data included in this paper are available on reasonable request.

Declarations

Conflict of interest: The authors have no competing interests to declare that are relevant to the content of this article.

Reference

[1] C. A. Blackshields and A. M. Crean, "Continuous powder feeding for pharmaceutical solid dosage form manufacture: a short review," *Pharmaceutical development and technology,* vol. 23, pp. 554-560, 2018.

[2] H. Tan, W. Shang, F. Zhang, A. T. Clare, X. Lin, J. Chen*, et al.*, "Process mechanisms based on powder flow spatial distribution in direct metal deposition," *Journal of Materials Processing Technology,* vol. 254, pp. 361-372, 2018.

[3] T. M. Francis, C. J. Gump, and A. W. Weimer, "Spinning wheel powder feeding device—fundamentals and applications," *Powder technology,* vol. 170, pp. 36-44, 2006.

[4] S. Yang and J. R. G. Evans, "Metering and dispensing of powder; the quest for new solid freeforming techniques," *Powder Technology,* vol. 178, pp. 56-72, 2007/09/05/ 2007.

[5] B. El Kassem, T. Brinz, V. Jenkouk, Y. Heider, and B. Markert, "Design of a vertical Loss-in-Weight feeder prototype with experimental proof of concept validation," *Pharmaceutical Development and Technology,* vol. 26, pp. 559-575, 2021.

[6] A. P. Shier, A. Kumar, A. Mercer, N. Majeed, P. Doshi, D. O. Blackwood*, et al.*, "Development of a predictive model for gravimetric powder feeding from an API-rich materials properties library," *International Journal of Pharmaceutics,* vol. 625, p. 122071, 2022/09/25/ 2022.

[7] A. Singh, S. Kapil, and M. Das, "A comprehensive review of the methods and mechanisms for powder feedstock handling in directed energy deposition," *Additive Manufacturing,* vol. 35, p. 101388, 2020.

[8] Z. Y. Chua, I. H. Ahn, and S. K. Moon, "Process monitoring and inspection systems in metal additive manufacturing: Status and applications," *International Journal of Precision Engineering and Manufacturing-Green Technology,* vol. 4, pp. 235-245, 2017.

[9] D. Minglani, A. Sharma, H. Pandey, R. Dayal, J. B. Joshi, and S. Subramaniam, "A review of granular flow in screw feeders and conveyors," *Powder Technology,* vol. 366, pp. 369-381, 2020.

[10] Q. Hou, K. Dong, and A. Yu, "DEM study of the flow of cohesive particles in a screw feeder," *Powder Technology,* vol. 256, pp. 529-539, 2014.

[11] D. Minglani, "Analysis of flow behavior of cohesive monosized spherical and non-spherical particles in screw feeder," *Powder Technology,* vol. 398, 2022.

[12] Unitrak.com. *Advantages and limitations of flexible screw conveyors*.

[13] F. J. C. Rademacher, "On the application of vibratory disk feeders for silos," *Forschung im Ingenieurwesen,* vol. 62, pp. 129-145, 1996.

[14] A. D. Ishkov, A. V. Stepanov, S. V. Miloradov, and I. V. Voronina, "Energy-efficient vibratory feeder of bulk construction materials," *Applied Mechanics and Materials,* vol. 670, pp. 458-461, 2014.

[15] S. Fathollahi, S. Sacher, M. S. Escotet-Espinoza, J. DiNunzio, and J. G. Khinast, "Performance evaluation of a high-precision low-dose powder feeder," *AAPS PharmSciTech,* vol. 21, pp. 1-13, 2020.

[16] O. Molerus, "Overview: pneumatic transport of solids," *Powder technology,* vol. 88, pp. 309-321, 1996.

[17] M. Nifuku and H. Katoh, "A study on the static electrification of powders during pneumatic transportation and the ignition of dust cloud," *Powder Technology,* vol. 135, pp. 234-242, 2003.

[18] P. Dunst, T. Hemsel, and W. Sextro, "Analysis of pipe vibration in an ultrasonic powder transportation system," *Sensors and Actuators A: Physical,* vol. 263, pp. 733-736, 2017.

[19] P. Dunst, P. Bornmann, T. Hemsel, and W. Sextro, "Vibration-assisted handling of dry fine powders," in *Actuators*, 2018, p. 18.

[20] R. Yu, X. Bai, X. Yu, and H. Zhang, "WC-reinforced iron matrix composites fabricated by wire arc additive manufacturing combined with gravity-driven powder feeding: particle transportation and size effects," *Rapid Prototyping Journal,* vol. 29, pp. 1014-1028, 2023.

[21] M. Jaklič, K. Kočevar, S. Srčič, and R. Dreu, "Granular Matter Transport in Vertical Pipes: The Influence of Pipe Outlet Conditions on Gravity-driven Granular Flow," *Acta Chimica Slovenica,* vol. 63, 2016.

[22] M. Moreno-Benito, K. T. Lee, D. Kaydanov, H. M. Verrier, D. O. Blackwood, and P. Doshi, "Digital twin of a continuous direct compression line for drug product and process design using a hybrid flowsheet modeling approach," *International Journal of Pharmaceutics,* vol. 628, p. 122336, 2022/11/25/ 2022.